

Influence of Annealing on Nanocrystal Formation in Ni Amorphous Alloy

G. N. Kozhemyakin^a, V. A. Shapovalov^b, Yu. A. Nikitenko^b,
O. N. Ivanov^c, D. A. Kolesnikov^c, and O. N. Maradudina^c

^a V. Dal Eastern Ukrainian National University, Lugansk, 91034 Ukraine
e-mail: genakozhemyakin@mail.ru

^b E.O. Paton Electric Welding Institute, National Academy of Sciences of Ukraine, Kiev, 03680 Ukraine

^c Belgorod State University, Belgorod, 308034 Russia

Received November 24, 2008

Abstract—An amorphous Ni alloy has been obtained as a ribbon by plasma-arc melt spinning in a copper water-cooled lining slag crucible. Ribbon samples have been annealed in a special cylindrical furnace at temperatures from 200 to 400°C for 1 h in Ar. It is established that nanocrystals in the alloy samples increase in size with increasing annealing temperature. The rise of resistivity upon annealing at temperatures below 300°C and its significant decrease at higher temperatures is consistent with the change in the amorphous alloy microstructure.

INTRODUCTION

Amorphous alloys have a high corrosion resistance. They are used to design and make electrode materials, fuel elements, filters operating in acid solutions and sewage, materials for soda production, etc. Amorphous alloys that are used as solders are of special interest [1]. It is known that annealing facilitates the crystallization of amorphous alloys and changes their properties [2–4]. Thus, the study of the temperature effect on the amorphous alloy microstructure is an urgent problem. In this paper, we report the results of studying the effect of annealing amorphous Ni–Si–B alloy on its microstructure and resistivity.

EXPERIMENTAL

We investigated an Ni alloy of the following composition (wt %): Ni (88), Si (7), B (3.5), Fe (0.5), Cr (1). The amorphous state was obtained as a ribbon by plasma-arc melt spinning in a copper water-cooled lining slag crucible. This preparation scheme was developed as an alternative to the classical spinning technique from ceramic crucible. The lining slag melting makes it possible to reduce the melt contact area with the ceramics and to prevent nonmetallic inclusions from penetrating in the melt, while the plasma-arc source has a large power margin and can superheat melt in a wide temperature range [5]. The mixture was prepared from the above-mentioned starting materials of 99.99% purity and placed in a copper water-cooled crucible with 110–140 mm inner diameter and 50 mm height. The heat source was a direct-action dc plasma-

tron with argon as a plasma-forming gas. The melt temperature during spinning was about 1100°C. After the mixture melting and stationary regime achievement, an excess pressure of 0.5 atm was formed very rapidly in the chamber, and the melt was squeezed out onto the disk surface through a ceramic nozzle fixed in the copper crucible bottom. The melt was spun onto a copper refrigerator disk with 300 mm diameter rotating at 1600 rpm. The amorphous alloy was a ribbon about 60 μm thick, 15 mm wide, and 30–40 m long. Samples 15 × 8 × 0.06 mm³ in size were cut from the ribbon, washed in acetone, and annealed in argon at temperatures from 200 to 400°C in a special cylindri-

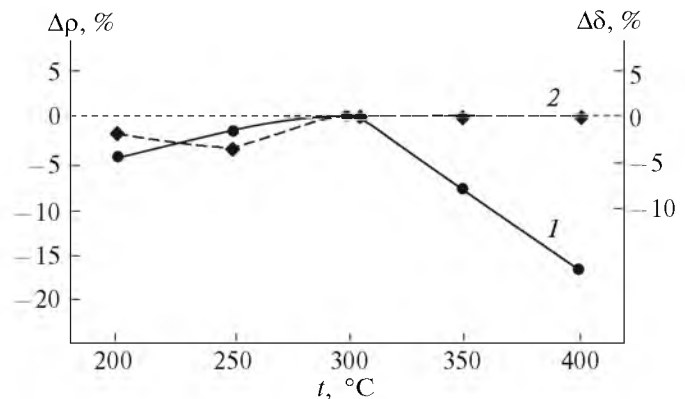


Fig. 1. Dependences of (1) the relative change on electrical resistivity, $\Delta\rho$, and (2) the thickness $\Delta\delta$ of amorphous alloy samples on the annealing temperature.

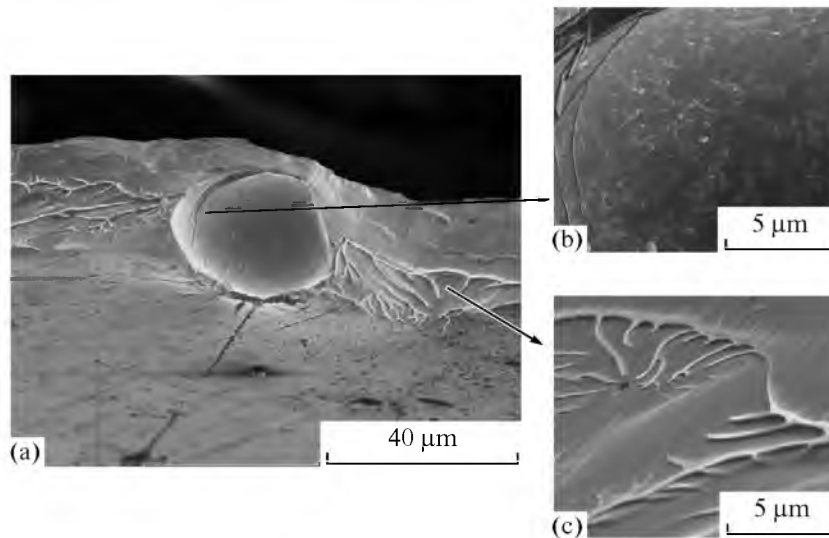


Fig. 2. Initial stage of amorphous alloy crystallization at 200°C annealing: (a) surface region, (b) nanocrystals in the spherical region, and (c) alloy flow with the formation of a wavelike relief.

cal furnace with a temperature gradient of no more than 1 K/cm in the axial and radial directions. The cross section surface was prepared by breaking the samples in liquid nitrogen, and the surface microstructure was studied in the scanning electron microscope “Quanta 200 3D”.

RESULTS AND DISCUSSION

It was established that the unannealed samples had not the micro- or nanocrystals either on the surface or in the cross section; i.e., the ribbon was amorphous throughout the bulk. A visual examination of the annealed samples did not reveal an oxide film on the surface. Annealing at 200 and 250°C was found to make the samples up to 3% thinner (Fig. 1). In addition, annealing at temperatures below 300°C led to a observable increase in the alloy’s resistivity, while higher temperature annealing significantly reduced this parameter; this may be caused by the change of the alloy microstructure. The 200°C annealing facilitates the surface region contraction due to the atomic diffusion, as a result of which the amorphous alloy “flows” or “relax” with the formation of a wavelike relief (Figs. 2a, 2b). This pattern is in agreement with the decrease in the sample thickness (Fig. 1). Thus the initial stage of crystallization process is realized. Then crystallization centers are formed either at surface defects or in the denser surface regions of the amorphous alloy. These centers evolve into nanocrystals, which can be seen well in the spherical region at the sample surface (Fig. 2c); most nanocrystals have a spherical shape and are from 10 to 640 nm in diameter. The increase of the annealing temperature to 300°C facilitated the nanocrystal growth (to more than 100 nm in size). This is clearly demonstrated by the

distribution pattern of the nano- and microcrystals in the sample cross section (Fig. 3). The nanocrystals from 10 to 84 nm sizes were observed in the ribbon surface region up to 10 μm depth. Their concentration and size decreased with the increase of the distance from the surface. The smallest nanocrystals were at a depth of more than 8 μm.

The ribbon surface contained protrusions, formed generally by the microcrystals concentrated near the surface. The microcrystals had an irregular (close to oval) shape and were from 220 to 680 nm in size. They are likely to be formed during annealing from the first nanocrystals nucleated at surface defects. The samples annealed at 300°C also observed the nanocrystals in the deformed regions (fractures typical of crystal failure) related to the sample breaking in liquid nitrogen (Fig. 4).

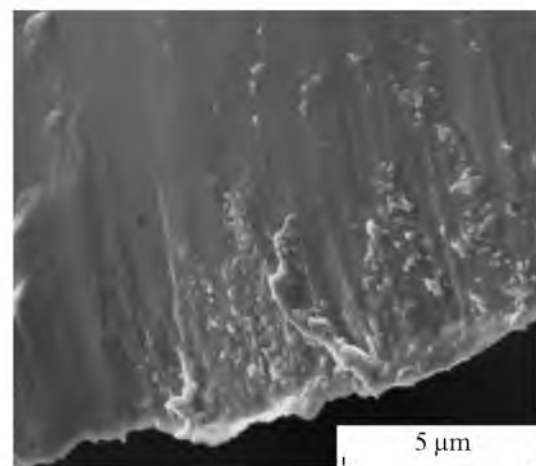


Fig. 3. Nano- and microcrystals at the surface of an amorphous ribbon annealed at 300°C.

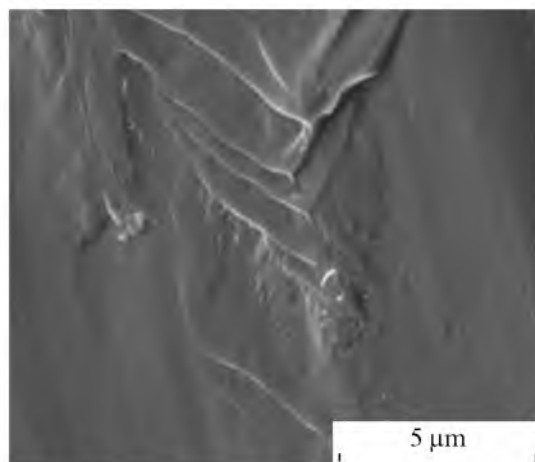


Fig. 4. Nanocrystals in the region deformed as a result of the alloy sample breaking in liquid nitrogen after annealing at 300°C.

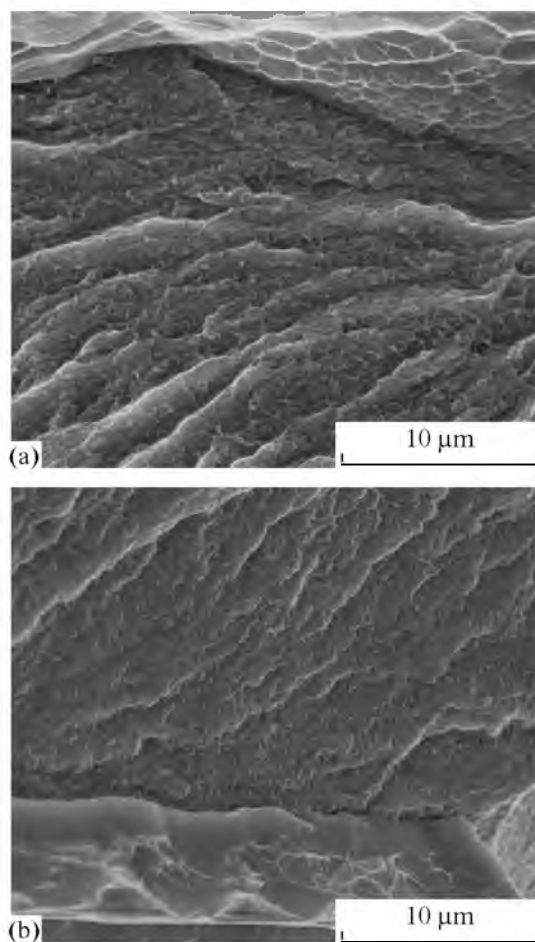


Fig. 5. Microstructure of the alloy samples annealed at (a) 350 and (b) 400°C.

The increase of the annealing temperature above 350°C, the alloy passes from the amorphous state to the crystalline state. A characteristic feature is the

wavelike arrangement of the microcrystals. After annealing at 350°C (Fig. 5a), the wavelike microcrystal regions are more pronounced than after 400°C annealing (Fig. 5b). We believe that this microstructure morphology forms due to the onset of nano- and microcrystal growth near the amorphous ribbon surface and their further propagation to the central part of the ribbon with simultaneous growth. As a result, (75–100)-nm nanocrystals and microcrystals up to 300 nm in size were observed in the central part of the cross section of the samples annealed at 350 and 400°C. The microcrystals in the surface regions of these samples were as large as a few micrometers. The largest (up to 7 μm) microcrystals were observed after annealing at 400°C. Such behavior of the microcrystal size with the increase in the annealing temperature is consistent with the decrease in the alloy electrical resistivity (Fig. 1).

CONCLUSIONS

A regularity in the formation of the nano- and microcrystals in amorphous Ni alloy during annealing at temperatures from 200 to 400°C for 1 h was established.

Annealing at temperatures below 250°C revealed the change of the amorphous ribbon thickness and increase of electrical resistivity, which are caused by the precrystallization transformation; the latter manifests itself as an alloy relax with the formation of a wavelike relief in the surface region. Annealing at 300°C leads to the formation of the nano- and microstructures with crystal sizes from 10 to 680 nm. The crystal nucleation begins on the ribbon surface, and the region of crystallization center formation expands to 10 μm depth during annealing. The nanocrystals are also observed in the alloy regions deformed during breaking in liquid nitrogen.

Nanocrystals 75–100 nm in size and microcrystals as large as 300 nm were observed in the central part of the cross section of the samples annealed above 350°C. The microcrystal sizes in the surface region of these samples reached 7 μm. A characteristic feature of these samples is the wavelike microstructure morphology throughout their cross section, which may be due to the onset of the nano- and microcrystal growth at the amorphous ribbon surface and their further propagation to the central part of the ribbon with simultaneous growth.

REFERENCES

1. B. A. Kalin, O. N. Sevryukov, V. T. Fedotov, and A. N. Plyushev, *Tekhnol. Mashinostr.* **4**, 45 (2003).
2. K. Lu, J. T. Wang, and W. D. Wei, *Scripta Metal. Mater.* **25** (3), 619 (1991).
3. N. I. Noskova, N. F. Vil'danova, A. P. Potapov, and A. A. Glazer, *Fiz. Met. Metalloved.* **73** (2), 102 (1992).
4. N. I. Noskova, E. G. Ponomareva, A. A. Glazer, et al., *Fiz. Met. Metalloved.* **76** (5), 171 (1993).
5. V. A. Shapovalov, Yu. A. Nikitenko, and V. R. Burnashev, *Sovrem. Élektrometall.*, No. 4, 12 (2004).

Translated by Yu. Sin'kov